Expert Opinion on Drug Delivery

ISSN: 1742-5247 (Print) 1744-7593 (Online) Journal homepage: http://www.tandfonline.com/loi/iedd20

The effects of particle size, shape, density and flow characteristics on particle margination to vascular walls in cardiovascular diseases

Hang T. Ta, Nghia P. Truong, Andrew K. Whittaker, Thomas P. Davis & Karlheinz Peter

To cite this article: Hang T. Ta, Nghia P. Truong, Andrew K. Whittaker, Thomas P. Davis & Karlheinz Peter (2018) The effects of particle size, shape, density and flow characteristics on particle margination to vascular walls in cardiovascular diseases, Expert Opinion on Drug Delivery, 15:1, 33-45, DOI: 10.1080/17425247.2017.1316262

To link to this article: https://doi.org/10.1080/17425247.2017.1316262

Accepted author version posted online: 07 Apr 2017.
Published online: 13 Apr 2017.

EXPERT OPINION ON DRUG DELIVERY, 2018
VOL. 15, NO. 1, 33–45
http://dx.doi.org/10.1080/17425247.2017.1316262

Taylor & Francis
Taylor & Francis Group

REVIEW

The effects of particle size, shape, density and flow characteristics on particle margination to vascular walls in cardiovascular diseases

Hang T. Ta[a,b], Nghia P. Truong[b,c], Andrew K. Whittaker[a,b], Thomas P. Davis[b,c,d] and Karlheinz Peter[e,f]

[a]Australian Institute for Bioengineering and Nanotechnology, University of Queensland, Brisbane, Australia; [b]ARC Centre of Excellence in Convergent Bio-Nano Science and Technology, Australia; [c]Monash Institute of Pharmaceutical Sciences, Monash University, Parkville, Melbourne, Victoria, Australia; [d]Department of Chemistry, University of Warwick, Coventry, UK; [e]Atherothrombosis and Vascular Laboratory, Baker IDI Heart and Diabetes Institute, Melbourne, Australia; [f]Department of Medicine, Monash University, Melbourne, Australia

ABSTRACT

Introduction: Vascular-targeted drug delivery is a promising approach for the treatment of atherosclerosis, due to the vast involvement of endothelium in the initiation and growth of plaque, a characteristic of atherosclerosis. One of the major challenges in carrier design for targeting cardiovascular diseases (CVD) is that carriers must be able to navigate the circulation system and efficiently marginate to the endothelium in order to interact with the target receptors.

Areas covered: This review draws on studies that have focused on the role of particle size, shape, and density (along with flow hemodynamics and hemorheology) on the localization of the particles to activated endothelial cell surfaces and vascular walls under different flow conditions, especially those relevant to atherosclerosis.

Expert opinion: Generally, the size, shape, and density of a particle affect its adhesion to vascular walls synergistically, and these three factors should be considered simultaneously when designing an optimal carrier for targeting CVD. Available preliminary data should encourage more studies to be conducted to investigate the use of nano-constructs, characterized by a sub-micrometer size, a non-spherical shape, and a high material density to maximize vascular wall margination and minimize capillary entrapment, as carriers for targeting CVD.

ARTICLE HISTORY
Received 9 January 2017
Accepted 3 April 2017

KEYWORDS
Particle physical properties; particle shape; particle size; particle density; flow characteristics; margination; cardiovascular diseases; atherosclerosis

1. Introduction

Despite significant clinical advances in the field, cardiovascular diseases (CVDs) remain the leading cause of death and disability worldwide [1–3]. They account for 17.3 million deaths per year, representing 30% of all global deaths, of which 80% take place in low- and middle-income countries [1]. Atherosclerosis, a chronic inflammatory disease of the vascular wall and a major cause of ischemic heart disease, is the most common form of CVD and the leading cause of sudden death. The process of atherosclerosis, which requires a complex interplay between various cells, particular monocytes, macrophages, and platelets [4,5], can ultimately lead to stroke, heart attack, angina, heart failure, and peripheral vascular disease. Once established, an atherosclerotic plaque can progress in two ways: the formation of either a stable plaque or an unstable, vulnerable plaque [6]. Unstable, vulnerable atherosclerotic plaques are prone to rupture and consequently can cause thrombosis, resulting in myocardial infarction and stroke [7].

Numerous studies have been undertaken in attempts to prevent, diagnose, and treat the often deadly complications of atherosclerosis. Among these, nanomedicine as an emerging field that utilizes nanotechnology concepts for advanced therapy and diagnostics has attracted major interest. It has been reported that the targeting of the plaques occurs via both the vasa vasorum and the main lumen at the lesioned sites [8,9]. Vasa vasorum is a network of small microvessels or capillaries entering the plaques from the opposite site. Similar to cancer, the key targeting principles in atherosclerosis can be divided into nonspecific targeting through the enhanced permeability and retention (EPR) effect and active targeting toward vascular cells or specific components within the plaques such as macrophages, lipoproteins, and cysteine proteases. EPR mainly occurs through the permeability of the microvascular systems or the leakiness of the neovessels of the vasa vasorum. While the effect of the physical properties of the nanomedicine on plaque targeting from the lumen site has been studied widely, the effect of these properties on plaque targeting via EPR in the vasa vasorum has been investigated limitedly. In this review, we focus on plaque targeting from the lumen site.

In the last decades, vascular targeting has been explored for localized delivery of therapeutics mainly in cancer [10,11], but also increasingly in cardiovascular and pulmonary diseases [12–14]. Vascular targeting plays a crucial role and is of particular interest for the diagnosis and treatment of atherosclerosis. This is because specific vascular wall endothelial cell receptors associated with acute and chronic inflammation, such as selectins, intercellular adhesion molecule 1 (ICAM-1), and vascular cell adhesion molecule 1 (VCAM-1), play a major

CONTACT Hang T. Ta h.ta@uq.edu.au; Karlheinz Peter karlheinz.peter@bakeridi.edu.au

Article highlights

- The physical characteristics of the particles are key factors in the design of carrier systems to target atherosclerosis from the main vessel lumen as they significantly affects carrier performance.
- Local hemodynamic conditions at the site of atherosclerosis also determine the extent of particle adhesion to the vascular walls.
- Microparticles display better adhesion than nanoparticles, regardless of shape. However, they are potentially susceptible to physical entrapment in the capillaries *in vivo*.
- Non-spherical particles exhibit higher adhesion than their spherical counterparts. Disks adhere to the vascular walls better than rods.
- There is a lack of thorough understanding of the side effects, degradation, and toxicity of non-spherical particles at different biological levels such as the body, organs, and cells.
- There is a clear need for thorough studies of the cellular uptake of particles of different size, shape, and density under different flow conditions, particularly those relevant to atherosclerosis
- The effect of particle's physical properties on atherosclerosis targeting from the vasa vasorum site should be thoroughly investigated

This box summarizes key points contained in the article.

role in the pathology of this disease and can therefore serve as local targeting epitopes [15].

One of the major challenges in carrier design for targeting CVDs from the vessel lumen is that carriers must be able to navigate the circulation system and efficiently marginate or localize to the endothelium in order to interact with the target receptors. Compared to nonspherical particles, spherical particles have been widely studied for targeting therapeutics to the vascular wall due to their ease of fabrication and the existence of well-defined models of hydrodynamic interactions [16–18]. Particles sized in the submicron down to tens of nanometers range are particularly attractive for intravenous delivery, since they can pass through the microcirculation with ease [17] and are less susceptible to immune recognition and consequent clearance [18,19]. However, in addition to the ability to navigate the circulatory system, the particles should be designed to drift laterally toward the vessel walls, like leukocytes during an inflammatory process, rather than moving within the core of the vessels, as red blood cells generally do in the macro- and microcirculation [20]. The benefit of a highly specific ligand–receptor targeting system is diminished if the particles cannot interact with the target endothelium due to suboptimal deposition. Recently, particles with nonspherical shapes [21,22] and micrometer sizes [15,23,24] have been increasingly recognized as better carriers for targeting CVD. Particle density has also appeared as an important factor affecting particle margination to blood vessel walls [23,25].

Furthermore, vascular-targeted carriers must remain bound long enough to release their drug cargo or to be internalized by the endothelial cells [23]. The interaction between the particle ligands and the cell surface receptors must be strong to overcome the shear force and momentum on the particle imparted by blood flow in order to result in firm adhesion. The characteristic forces ascribed to blood flow dynamics (hemodynamics) are a crucial element in the adhesive interactions of vascular-targeted carriers with the endothelium, as hemodynamics is known to be important for the binding of leukocytes (white blood cells [WBCs]) with the endothelium – a hallmark of the natural immune response. Therefore, hemodynamics must be an important consideration in the design of vascular-targeted drug carriers. Here, we review the effects of physical characteristics of therapeutic carriers including size, shape, and density, along with hemodynamics on the ability of vascular-targeted drug/imaging carriers to marginate (localize and bind) to the vessel wall.

2. Blood flow in the presence of atherosclerosis

Blood is a complex aqueous fluid containing plasma (different molecules and proteins) and cells including red blood cells (RBCs), WBCs, and platelets [26]. Hemodynamics (particularly blood shear rate and vessel size) and hemorheology (blood rheology or blood hematocrit) are known to be important factors in the interaction of WBCs with the endothelium *in vivo* [26,27]. WBCs (8–12 μm diameter) are nearly twice as large as RBCs, while platelets (1–3 μm diameter) are around three times smaller than RBCs. Size and other physical properties of RBCs (shape and deformability) allow them to be preferentially confined within the core/center of the blood vessels [28], forcing the other blood cells (WBCs and platelets) into an almost RBC-free layer (RBC-FL) of plasma located toward the vessel wall, thus promoting the interaction of WBCs and platelets with the endothelium [29–32] .

The blood flow pattern changes during the development of atherosclerosis [33]. Understanding blood flow is important for the design and engineering of an optimally targeted vascular nanoparticle for atherosclerosis. The extent of blood flow within a vessel is directly proportional to pressure gradients and inversely proportional to vascular resistance. Small changes in vessel diameter due to a growing atherosclerotic plaque can lead to substantial changes in vascular resistance, thus changing the flow pattern significantly. Blood flow is known to have a laminar pattern characterized by a parabolic flow profile (Figure 1, left and right) [33,34]. When blood flow transitions from a laminar, parabolic flow to a turbulent flow, the blood flows across the vessel (no longer along it), and vortices are formed which significantly increase the overall flow resistance (Figure 1, middle). Turbulent/recirculating flow, a direct function of blood velocity and inversely related to viscosity, occurs when there are changes in the structure of a vessel, such as an obstruction (Figure 1, middle), a sharp turn, or a rough surface [35,36]. In laminar flow, the wall shear stress is high while in disturbed flow it is lower. The areas of the vasculature prone to developing atherosclerotic changes tend to be large vessels and exhibit disturbed blood flow profiles [37], including high pulsatility (regulated by the cardiac cycle), low net shear due to reverse flow, and recirculation eddies near areas of bifurcation or high curvature [38].

3. The role of particle size along with hemodynamics and hemorheology

Atherosclerotic plaques preferentially develop at bifurcations of blood vessels where disturbed flow and streamline separation occur [24]. It has been shown that particle size and hemodynamics affect the adhesion of particles to endothelium synergistically. Generally, the binding of particles from blood flow to

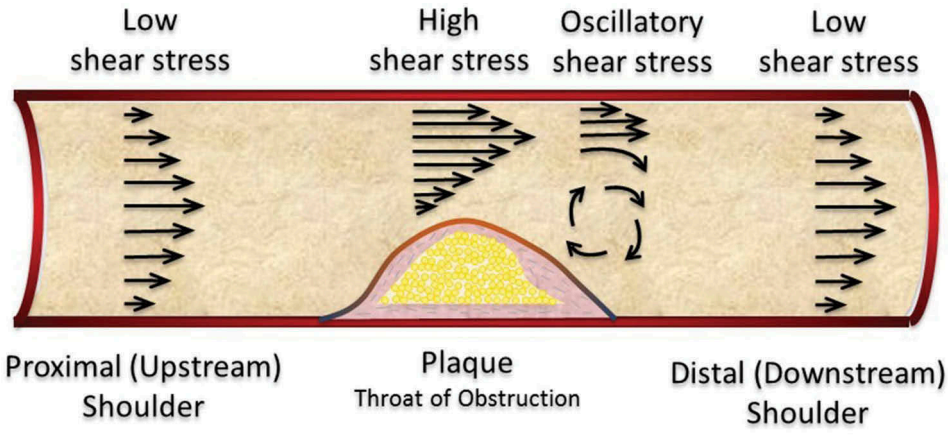

Figure 1. Baseline endothelial shear stress patterns along the course of a coronary artery obstruction.

the inflamed endothelium generally increases with increasing particle size, hematocrit, and wall shear rate (WSR).

3.1. Particle size

Charoenphol et al. found that the binding efficiency of polymeric spheres to the inflamed endothelium from laminar flow of reconstituted blood (RBCs in homologous plasma with no leukocyte or platelets) *in vitro* via parallel plate flow chamber (PPFC) assays generally increased with increasing particle size from 100 nm up to 10 μm [23]. These polymeric spheres were functionalized with sialyl Lewis^A (sLe^A), a carbohydrate ligand specific to the endothelial-expressed selectins. In another study, carboxylate-modified polystyrene spheres were functionalized with sLe^A, human ICAM-1 antibody (aICAM), or human VCAM-1 antibody (aVCAM), which targeted molecules overexpressed on the inflamed vascular wall [24]. Using *in vitro* PPFC, these authors also found that the efficiency of particle binding in disturbed and recirculating flows with reconstituted blood increased as the spherical diameter increased from 500 nm to 5 μm. Disturbed flow includes pulsatile flow, which is regulated by the cardiac cycle, and recirculation flow, which occurs in areas with sudden flow expansion in the arterial tree. Recirculation flow redistributes particle localization to the wall proximity, which increases the opportunity for particle binding far downstream [24]. Nano-sized particles showed minimal adhesion to the endothelium from blood flow in horizontal (gravity and antigravity directions) and vertical channels when compared to micron-sized spheres in all flow types (laminar, disturbed/pulsed, and recirculating) [23,24,27]. The channels used were on the order of small- to medium-sized venules and arteries. This can be explained by the poor ability of the nanoparticles from midstream to localize to the wall region [27] since they were strongly entrapped within the RBC core that forms when blood flows [39]. No significant difference was observed between the adhesion of 200 and 500 nm spheres [24]. In a mouse model of atherosclerosis, it was also found that 2 μm spheres displayed 2.5–3.5 times greater adhesion to the aortic wall than 500 nm spheres [24]. This *in vivo* adhesion difference between nanospheres and microspheres agrees well with observations from *in vitro* assays using human blood [24].

These results are consistent with data from Namdee et al. [15]. Using a mouse model of atherosclerosis, they demonstrated that the adhesion of dual-targeted (E-selectin and VCAM-1) 2-μm polystyrene particles to the inflamed aorta was greater than that of their 500 nm counterparts (at least fourfold) [15]. The adhesion was minimal for nanoparticles throughout the aorta compared to microparticles, even in areas where very high levels of inflammation were expected [15]. These results suggest that micron-sized spherical particles (2 μm), rather than nanospheres, are better for vascular-targeted drug delivery applications in medium to large vessels relevant in atherosclerosis. Particles with shapes other than spheres, such as disk-like and rod-like particles, also exhibit the same behavior where a larger size increases the binding efficiency [38,40]. For example, in PPFC assays with reconstituted blood flow, rod-like particles with 2-μm equivalent spherical diameters (ESDs) displayed higher margination than particles with either 1 μm or 500 nm ESDs [38]. In another study, larger rods (1800 × 400 nm) were observed to adhere at least three times more than smaller ones (1500 × 200 nm) [40]. This can be explained by the higher drag or higher settling velocity of larger particles compared to smaller ones. Nanorods (500 nm ESD), even with high aspect ratios (ARs, ratio between major axis and minor axis), did not display enhanced margination compared to that of equivalent spheres [38]. This indicates that, like nanospheres, nanorods display minimal margination due to their inability to effectively localize to the vessel wall in blood vessels or confined channels *in vitro* [38]. There are limited reports on the influence of the size of the disks on their binding efficacy. Disks of intermediate size (1000 × 400 nm) exhibited maximum adhesion compared with disks of larger size (1800 × 600 nm) or smaller size (600 × 200 nm), which reflects the balance between adhesive interfacial interactions and hydrodynamic dislodging forces [40].

3.2. Size and hematocrit

It is widely known that RBCs play a crucial role in the margination of leukocytes and platelets. RBCs either promote or hinder particle adhesion to endothelial cells in a PPFC depending on the blood flow pattern, hematocrit, and particle size [41]. The higher the hematocrit, the thinner the RBC-FL, resulting in more frequent collisions between spheres and RBCs, and so

enhancing the lateral migration of spheres toward the walls and promoting higher adhesion [41,42]. This explains the increased binding at higher hematocrit observed for 0.5-μm and 2-μm sLe^A-coated polystyrene spheres in reconstituted blood [41,42].

The same trend has been observed for both laminar flow with WSR of 500 s^{-1} (the median of values measured in human microvessels [43]) and pulsatile flow with peak WSR of 1000 s^{-1} (the typical pulsatile flow found in certain regions of the large arteries relevant in atherosclerosis [37]) [41]. However, the higher hematocrit did not enhance the binding of smaller (0.2 μm) or larger spheres (5.7 and 10 μm) [41]. In recirculating flow (WSR = 200 s^{-1}) via a vertical-step flow channel (VSFC), there was no difference in the adhesion of all spheres in the recirculation zone, while beyond flow reattachment, only 2 μm and 5.7 μm spheres saw significant increases in their binding levels with an increase in hematocrit, which differs from what has been observed in other flow types [41]. This is possibly due to the unique particle–RBC collision dynamics known to exist in recirculating flow. The lack of a hematocrit effect on the adhesion of 0.2 μm spheres across all flow types may be due to their significantly larger RBC-FL-to-particle-diameter ratio [41].

In a microcirculation setting with WSR of 200 s^{-1} (postcapillary venules [43,44]) and channel height of 254 μm (human arterioles and venules [43,44]), the presence of RBCs also enhanced the adhesion of sLe^A-coated neutrally buoyant spherical microparticles (≥2 μm diameter) to activated endothelial cells from reconstituted blood flow [17,23]. The binding efficiency for all particle sizes was further enhanced in disturbed whole blood flow compared to reconstituted blood flow [24]. This is likely due to the difference in hematocrit level between the whole blood and the reconstituted blood of ~45% and 30% hematocrit, respectively. Particles in the size range of 100–500 nm are not preferentially distributed to the vessel wall via the RBC effect, resulting in their low binding to endothelium in the presence of physiological levels of RBCs [23,26,27,38]. Small particles (≤100 nm) tend to circulate along with RBCs and only a small fraction interacts with the vessel walls [26], thus exhibiting minimal margination from bulk blood flow [45,46].

3.3. Size and channel orientations

No significant difference was observed in adhesion levels between adhesion in upward and downward flow for all particles tested in a vertical chamber [23]. The magnitudes of particle binding in the horizontal channel and inverted horizontal channel were almost the same [23]. This indicates that there is a minimal contribution of gravity to particle localization to the vessel wall. There was also no significance in the magnitudes of particle adhesion to the wall observed between vertical and horizontal chambers [23,24,47]. However, there was a significant decrease in the adhesion observed for large particles (5 and 10 μm) in the inverted versus the horizontal chamber, which can be explained by potential differences in the characteristics of the RBC-FL between the top and bottom of the PPFC [23]. Reports in the literature have shown that the average plasma layer thickness can differ significantly between the top and bottom wall in a horizontally aligned channel *in vitro* or a blood vessel *in vivo* [48,49].

3.4. Size and WSR

The adhesive behavior of the particles depends on the magnitude of the WSR. In a PPFC system with laminar reconstituted blood flow at 200 s^{-1}, the level of particle adhesion increased with increasing particle size [23]. When the WSR was increased to 500 s^{-1}, the adhesion increased only when the particle size also increased from 0.5 up to 5 μm. The adhesion of 10 μm spheres at this WSR was significantly lower than those measured for 2 and 5 μm particles. Further increases in WSR to 1000 s^{-1} and 1500 s^{-1} resulted in adhesion only increasing with a concomitant increase in particle size from 0.5 to 2 μm. Particle sizes beyond 2 μm at these WSRs resulted in the same or significantly lower level of binding than displayed by 2-μm particles. It appears that for particles ≥2 μm, there is a critical WSR (WSR_{crit}) at which the binding increases with increasing WSR up to WSR_{crit}, then drops with WSR beyond the WSR_{crit}. This drop is due to the higher disruptive hemodynamic forces interfering with particle adhesion, rather than ineffective particle localization to the wall [23]. Overall, the magnitude of the WSR_{crit} decreased as the particle size increases from 2 to 10 μm. Nanospheres do not have a critical WSR: particles <2 μm display minimal adhesion for all WSRs.

This coupling effect of size and WSR on the adhesion of polymeric spheres has also been reported by Shinde Patil et al. [50] and can be explained by (1) the transport of particles to the vessel wall, typically regulated by convection and diffusion; (2) the reaction between particle ligands and cell surface receptors, controlled by receptor–ligand density and particle slip velocity [51]; and (3) the detachment of particles, regulated by WSR and the reverse reaction rate [52]. Similarly, in a microfluidic model of human microvessels employing 28 and 43 μm channels, the binding of nanospheres did not significantly change with increases in WSR from 100 s^{-1} to 500 s^{-1} in both microchannels. However, unlike what has been observed with the PPFC system, the adhesion efficiency of microspheres in microchannels did not increase with increasing WSR [27]. In particular, for 2-μm polystyrene spheres, the adhesion efficiency slightly decreased with an increase in WSR from 100 s^{-1} to 200 s^{-1} in the 43 μm channel, while it did not change with any increases in WSR in the 28 μm channel. For 5 μm spheres, the adhesion efficiency significantly decreased for all WSR increases in both channels and was much lower than that of 2 μm spheres due to the high slip velocity and higher disruptive force associated with large-sized particles [27].

3.5. Size and channel height

Adhesion assays in horizontal chambers with varying channel height at a fixed WSR of 200 s^{-1} showed that adhesion of spherical particles decreased with increases in channel height from 127 to 762 μm for all particles sizes studied [23]. This decrease in binding efficiency may be due to a reduction in

the contribution of the RBC-generated force normally acting at larger channel heights. The size of the RBC-FL in humans has been reported to be between 2 and 10 μm depending on the vessel size, WSR, and blood hematocrit [53,54]. At a fixed hematocrit, the RBC-FL thickness increases with an increase in vessel diameter; therefore, there is less RBCs–particle interaction near the wall [48,53,54]. Similarly, in a microfluidic model of human microvessels, adhesion efficiency was higher in the 28 μm channel relative to the 43 μm channel for all spheres (0.2–5 μm), although these increases were only significant for microspheres [27].

3.6. Size and flow type

The introduction of pulsatility and/or recirculation to flow did not alter the adhesion trends seen as a function of particle size when compared to the adhesion trend in laminar flow with equivalent WSR [23,24]. Particle adhesion increased as particle size increased from 0.5 to 5 μm. No difference in adhesion was observed between 0.2 and 0.5 μm spheres. sLe^A-polystyrene microspheres displayed significantly higher adhesion levels in both pulsatile flow (WSR = 1000 s^{-1} and 1200 s^{-1}) and recirculating flow (WSR = 200 s^{-1} and 500 s^{-1}) than their counterparts in laminar flow at the same WSRs [24]. The adhesion of nanospheres was not enhanced with pulsatility in flow [23,24]. An increase in microparticle adhesion directly correlates with an increase in the residence time of particles with pulsatile flow relative to laminar flow, suggesting that increased residence time is likely the major factor contributing to adhesion increase under pulsatile flow [24]. Pauses in flow lead to periods of low slip velocities for large particles and thus better opportunity for adhesion. The adhesion of nanospheres was similar in the presence or absence of pulsatility in flow, since there are minimal hemodynamic/disruptive forces acting on nanoparticles compared to microspheres, and thus, their adhesion will be minimally affected by pauses in flow [55].

The binding of polystyrene microspheres in recirculating reconstituted blood flow in a VSFC (Figure 2(a,b)) (WSR = 200 s^{-1} and 500 s^{-1}) exhibited an adhesion profile which peaked in the reattachment area, just beyond the reattachment point (Figure 2(c,d)), due to low parallel shear forces and a maximum normal velocity on the wall [56], consistent with previous reports of platelet (~2 μm) and leukocyte (~7–15 μm) adhesion in similar VSFC [56,57]. The adhesion of all spheres in the far downstream region (laminar flow regime [56]) was significantly higher than in laminar flow in PPFC with the same height and WSR [24]. Pulsatile flow in the VSFC did not enhance adhesion when compared with adhesion in laminar flow at the same average WSR in the VSFC, likely because pulsatile flow disrupts the particle distribution associated with recirculation flow [24].

In a mouse model of aorta atherosclerotic plaque, the binding of dual-targeted sLe^A/aVCAM-spheres was not

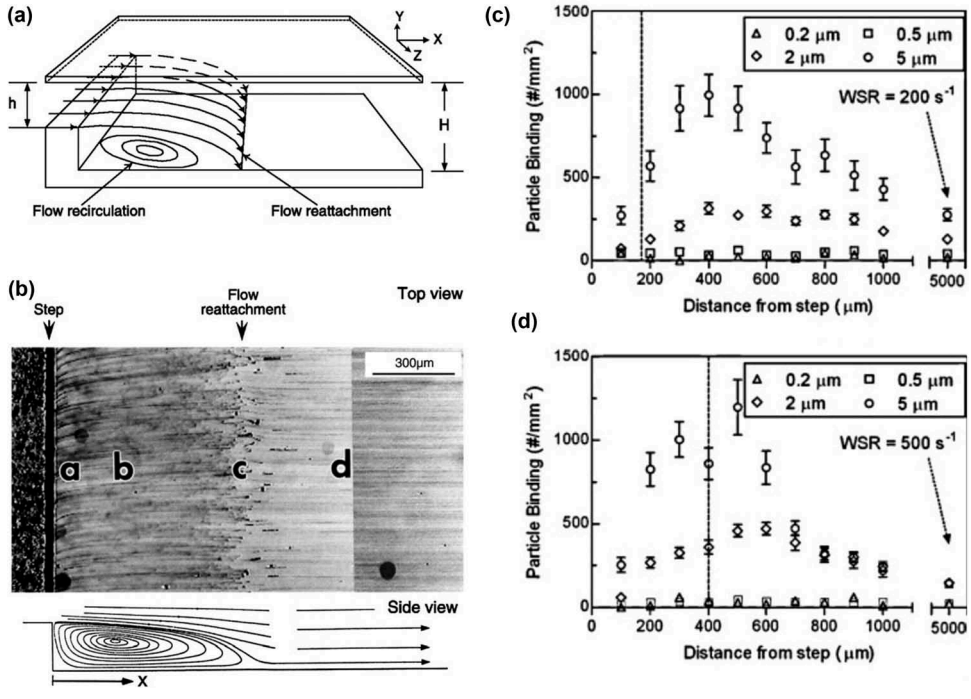

Figure 2. Visualization of flow patterns created in a vertical-step flow channel (VSFC) and typical adhesion profiles of microspheres in VSFC. (a) Schematic diagram of the flow channel showing the flow pattern immediately beyond the step: h and H are the heights of the channel above the step and beyond the step, respectively. (b top) Phase-contrast photomicrograph (top view) of experimental flow patterns in the VSFC. Flow is from left to right and is made visible with 1 μm marker microparticles. Flow separation occurs in the region distal to the step, forming four specific flow areas: a, the stagnant flow area; b, the center of the recirculation eddy; c, the reattachment flow area; and d, the fully developed flow area. From online microscopic observations, the particles transported from the bulk flow along the curved streamlines with decreasing velocities toward the wall near the reattachment point (area c). While some of the particles moved forward to rejoin the mainstream with increasing velocities, others moved in a retrograde direction toward the step as recirculation eddies. These latter particles moved upstream initially with increasing velocities, and decelerated when approaching the wall of the step (area a), from where they were carried away from the floor of the chamber by upward curved streamlines. (b bottom) Schematic drawing of the side view of the streamlines in the VSFC deduced from the top-view photograph. (c & d) sLeA-coated spheres binding in the VSFC with reconstituted blood flow. Far downstream conditions are 200 s¯1 and 500 s¯1 of laminar WSR, respectively. The dashed lines represent the observed reattachment points. Reproduced with permission from references [58] and [24].

significantly altered between different segments except in the iliac vessels [24], most likely due to their smaller lumen diameters. However, it is difficult to interpret these *in vivo* data due to the absence of detailed knowledge of local *in vivo* expression patterns, WSRs, and blood flow patterns in the different vessel segments [24].

Recirculating flow as well as pulsatile flow also enhanced the adhesion of microrods and did not alter the adhesion trend seen as a function of particle size [38]. The adhesion of rods with larger sizes was greater in all areas of the flow, including the recirculation region, reattachment/stagnation point, and far downstream area. There was no significant difference in the binding of short rods, such as 2-μm ESD rods with ARs of 2 and 4. The adhesion of 500-nm ESD rods in recirculating and pulsatile flows was minimal, which is similar to what has been observed in laminar flow [38].

Overall, the above data indicate that microparticles, especially 2–5 μm spheres and 2-μm ESD rods, are optimal for targeting the wall in the medium to large vessels relevant in several CVDs. Spheres with diameters in the 2–5 μm range display significantly better margination to the wall at intermediate to high WSRs and channel heights than the nanometer-sized spheres. Nanoparticles have much lower margination efficiency in disturbed human blood flow and thus may be more challenging for use as drug carriers or imaging probes in the treatment of atherosclerosis. Results from pulsatile flow assays may be relevant in diseases affecting the straight segments of medium to large arteries, e.g. peripheral artery disease and atherosclerosis, while recirculating flow is relevant around the branching points and curvatures in large arteries where atherosclerosis preferentially develops [34]. The results with laminar flow may be relevant in the main arterioles (~100–250 μm diameter) feeding a solid tumor [59].

4. The importance of shape

Due to the limited availability of techniques to produce nonspherical biocompatible nanoparticles [60], the majority of particles used in drug delivery are those with spherical shape [61]. However, carrier shape has been shown to have a profound effect on cellular internalization [62–65], circulation half-life [66,67], and margination toward the vessel wall [21,22], all of which directly affect the targeting ability of carriers [68]. Compared to spherical particles, nonspherical particles (Figure 3) appear to have advantages with respect to circulation and binding efficiency.

4.1. Macrophage uptake and circulation in the blood

Rod-like and disk-like particles are able to circulate in the blood for longer periods of time than spherical particles [61]. Along with other physicochemical properties such as nanoparticle size, surface charge, and surface functionality, shape significantly influences particle uptake by macrophages [62,69] and mammalian cells [67,70,71]. Rod-shaped nano- and micro-particles of different materials such as polystyrene, gold, and silica have been found to be endocytosed and cleared by macrophages of the liver and spleen to a lesser degree compared to spherical particles [62,64,65]. Similarly, disk-shaped particles such as elliptical polystyrene disks remain in the circulation for longer periods of time than

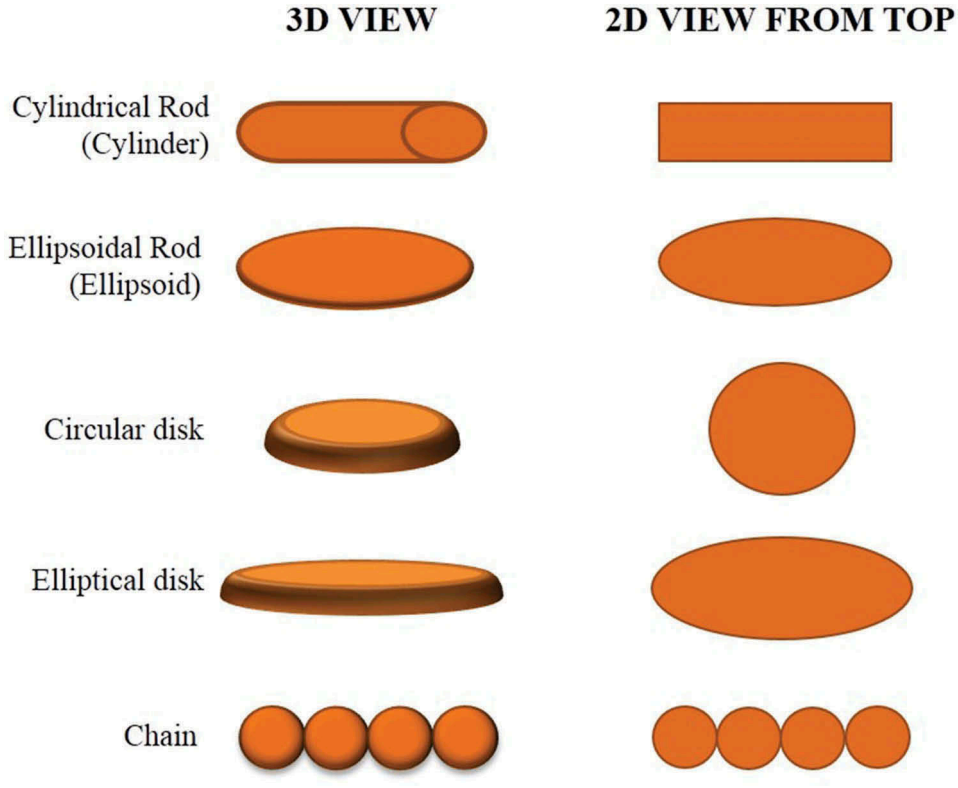

Figure 3. Schematic showing differently-shaped non-spherical particles investigated for vascular wall margination.

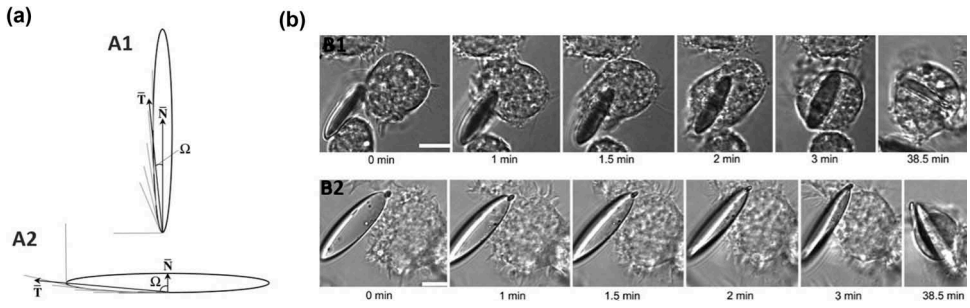

Figure 4. Local shape illustration and macrophage uptake of elliptical disks. (a) Schematic diagram illustrating how local shape is defined. T? represents the average of tangential angles near the point of cell contact. Ω is the angle between T? and the membrane normal at the site of attachment, N?. A1, Ω = 2.5° for cell attachment at end of worm. A2, Ω = 87.5° for cell attachment on side of worm. Reproduced with permission from reference [69]. (b) Time-lapse video microscopy clips spanning 39 min of macrophages interacting with identical non-opsonized elliptical disk (ED) particles (major axis 14 μm, minor axis 3 μm) from two different orientations. B1, cell attaches along the major axis of an ED and internalizes it completely in 3 min. B2, cell attaches to the flat side of an identical ED and spreads, but does not internalize the particle. Continued observation indicated that this particle was not internalized for >110 min. (scale bars: 10 μm). At least three cells were observed for each orientation of each particle type and size. Similar results were observed in all repetitions. Reproduced with permission from reference [62].

their spherical counterparts [67]. This explains the lower accumulation of rods and disks in the liver and spleen.

Macrophages internalize particles via actin-driven movement of the macrophage membrane, which is independent of surface chemistry and depends only on the local particle shape where the cell attaches [62]. Local particle shape, at the point of cell attachment, has been defined as the angle between the membrane normal at the point of initial contact and tangent lines drawn to the particle contour near the point of initial contact (Figure 4). Local shapes that have low length-normalized curvature (local particle shape $\Omega > 45°$, where 45° is the value for spherical particles) inhibit internalization, while spheres and local shapes that have high length-normalized curvature ($\Omega \leq 45°$) permit internalization [62]. Rods or worm-like particles with very high ARs (large Ω) inhibit or significantly reduce phagocytosis, as demonstrated by Champion et al. [69]. These authors have shown that worm-like polystyrene particles with very high ARs (>20) exhibited negligible phagocytosis compared to conventional spherical particles of equal volume. Internalization was possible only at the end points of the worm-like particles, while attachment anywhere along the length of the particles inhibited internalization due to the low curvature [69].

Recently, Liu et al. have also reported that tobacco mosaic virus (TMV) short rods with ARs of 4 and 8 were internalized much faster than TMV with the AR of 17 [72]. Huang et al. have also shown that the clearance rate of mesoporous silica nanoparticles (MSNs) is primarily dependent on the particle shape, where short-rod MSNs (AR 1.5, length 185 ± 22 nm) have a more rapid clearance rate than long-rod MSNs (AR 5, length 720 ± 65 nm) [64]. Due to their lower clearance rates, rod-like and disk-like particles appear to circulate in the blood for longer than spherical particles, which may contribute to their higher vascular targeting.

4.2. Vascular wall margination and attachment

Under microvascular blood-free flow conditions at low WSRs (<250 s^{-1}, physiological shear rates observed in the microcirculation), the adhesion of anti-bovine sreum albumin (BSA) neutrally buoyant polystyrene [73] and non-targeted mesoporous silicon [40] particles with different shapes (including spheres, elliptical/circular disks, and rods) to BSA- and collagen-coated flow chambers, respectively, was investigated. Rods provide information on the importance of elongation, and circular disks help determine the importance of flatness, whereas elliptical disks represent a combination of elongation and flatness. Under disturbed flow conditions, the adhesion of microparticles of any shape was significantly greater compared to that under laminar flow [73]. Rod-shaped particles exhibited significantly higher attachment compared to spherical particles, and the effect of shape was amplified by an increase in particle size [40,73].

Another study has also shown that non-neutrally buoyant silicon elongated microparticles exhibited a higher margination tendency compared to silica spheres irrespective of size and density under low WSRs (5–50 s^{-1}) [74] due to their lower drag and higher contact surface area compared to spheres. For particles of equal volume even in the nanometer ESD range, disks adhered about two times more than rods [40]. This can be explained by the slightly larger hydrodynamic forces exerted over the rods than those on the disks; the larger surfaces for adhesion exposed by the disks compared to long rods; and the higher rotational inertia on the rods compared to the disks. These results show that flatness, elongation, and adhesion surface area, as well as orientation during particle–wall interactions, are critical for firm particle adhesion. However, compared to flatness, elongation and adhesion area are the dominant factors for adhesion [40,73]. These data suggest that thin, disk-like particles could more effectively target diseased microvasculature as compared to spheres and slender rods.

These studies, however, did not examine binding efficiency between the endothelial cells and the ligands specific for these cells. In addition, the WSRs investigated in these studies were those of the microcirculation present in the vasculature embedded within organ tissues, tumor, or metastasis [75], which does not represent the circulation in arteries, where atherosclerosis can exist. Larger WSRs (>100 s^{-1}) are typically found in the microcirculation of healthy tissue, whereas lower values are relevant to tumor microcirculation (<100 s^{-1}) [76]. Employing the same concept, iron oxide nanochains have

been developed and constructed from three to four nanospheres covalently linked together for microvascular targeting in the diagnosis and treatment of cancerous and metastasis diseases [77–83]. However, there have been no reports on the use of nanochains in atherosclerosis.

Currently, there has been only one report on the effect of shape on the adhesion of targeted particles to activated endothelial cells in blood flow *in vitro*. Thompson et al. investigated the effects of particle shape parameters (volume, AR, and axis length) on the margination efficacy of targeted sLe^A-polystyrene spheres and prolate ellipsoids (rods) to an inflamed endothelial wall from human blood flow in an *in vitro* model of human vasculature, PPFC system, using reconstituted blood with laminar flow and disturbed flows, including pulsatile and recirculating flows, at a range of physiological WSRs (120–1200 s^{-1}) [38]. Rod-shaped microparticles (1or 2 μm ESD) with high ARs (9 and 11) displayed significantly improved margination compared to spheres of equal volume, particularly under high WSRs and disturbed flow profiles. The higher the AR or the longer the major axis, the better the adhesion of the rods, especially at high WSR (500–1000 s^{-1}) [84,85]. In disturbed flows such as pulsatile and recirculating flows, similar trends of adhesion were seen as in steady laminar flow. Nanorods (500 nm ESD), even with a high AR such as 10, do not display enhanced margination compared to equivalent spheres. It has been shown that a minimum major axis length for rods, rather than a minimum AR, is required for enhanced transportation to the wall, much like it has been shown that a minimum particle diameter (~2 μm) is required for the effective margination of spheres [86]. In this study, it was shown that the minimum major axis length is 5.9 μm [38]. Using modeling, Decuzzi et al. also predicted that the lateral drift velocity of discoidal microparticles increases (i.e. they undergo faster collisions with the wall) with increased particle elongation/major axis [87]. Due to limitations in current rod-fabrication techniques [88], it was not possible to fabricate rods of 500 nm ESD with a major axis greater than 2.5 μm, thus limiting the capacity to test this hypothesis for nanorods [38].

In a mouse model of atherosclerosis, dual-targeted polystyrene microrods (2 μm ESD) also displayed significantly higher adhesion densities than polystyrene microspheres (2 μm), while nanorods displayed no increased adhesion compared to equivalent 500-nm diameter spheres [15]. Among targeted rods of three different ARs (2, 4, and 9) with 2 μm ESD, the adhesion of the AR4 rods was the highest (~3 times higher) relative to the equivalent microspheres [15]. The adhesion of the AR2 and AR9 rods was roughly the same as for 2 μm spheres and lower than that of the AR4 rods. This differs from what has been observed *in vitro* where AR9 rods exhibited higher adhesion compared to AR2 and AR4 rods [38]. This is likely because of the relatively small difference in local shape and surface area between AR2 rods and spheres. The lower adhesion of AR9 rods compared to AR4 rods, despite their higher contact surface area, is likely due to their entrapment in the capillaries as AR9 rods have a major axis length of roughly 9 μm [15]. Recently, Wen et al. have also demonstrated that rod-shaped particles (elongated TMV) functionalized with binding peptides and contrast agents (gadolinium) could be targeted to activated platelets/thrombus in mouse carotid artery at a higher magnitude compared to sphere-like particles (icosahedral cowpea mosaic virus) [89].

Overall, nonspherical particles are more appropriate than spherical beads as carriers for targeting to the vascular walls under flow. Oblong particles exhibited higher adhesion magnitudes than their spherical counterparts. This can be explained by the longer circulation of oblongs in the blood compared to spheres. In addition, elongated particles are subjected to torque forces within blood flow, and therefore, they have a tendency to tumble out of the general circulation and scavenge along vessel walls [40,73,77,87] (Figure 5(a)). Spherical particles, on the other hand, tend to follow the streamlines. Furthermore, experimental and computational modeling data show that spherical microparticles experience the largest dislodging forces and exhibit the smallest areas of adhesion, followed by rods and then disks. Particle elongation and flatness increase the particle surface area in contact with the endothelium and thereby present a greater number of targeting ligands to the endothelium in cases where all particles have a fixed ligand density, as illustrated in Figure 5(b). This is because their ligands are arranged on a planar surface and available in greater numbers, in comparison to spherical particles where curvature limits the number of ligands available for binding in a given instance [90,91]. The higher contact area with the endothelium exhibited by rods and disks distributes their adhesive force over a larger surface area, and therefore a higher shear force required to remove an adherent particle from the vascular surface.

The streamlined shape of rods and disks also reduces the removal force due to the blood flow felt by these particles at the endothelium compared to an equivalent sphere [35]. The drag force exerted over a rod or disk is orientation dependent, and it reaches a maximum for a rod/disk lying with its major axis orthogonal to the flow. Disks and rods aligned with the flow experience the lowest drag force. For the hydrodynamic torque *T*, small variations were observed among the different particles [40]. Oblong particles aligned with the flow direction or immersed in a shear flow near a wall rotated more slowly compared to spherical particles [92]. In addition, the effect of the wall leads to several viscous interactions that do not exist for spherical particles. Therefore, nonspherical particles are able to adhere more strongly to the vascular wall.

However, these interactions disappear for oblong particles with very small ARs [92]. The lack of improved adhesion of nanorods compared to nanospheres is likely due to the general inability of nanoparticles to preferentially segregate to the RBC-FL and the diminished impact of a higher contact surface area on adhesion for these particles. However, nanodisks in low shear buffer flows exhibit around twofold greater adhesion over rods of equal volume, most likely due to slightly higher hydrodynamic forces exerted on the rods compared to disks and the larger surfaces for adhesion exposed by disks relative to rods [40]. However, the differences in binding of rods and disks to endothelial cells have not, however, been investigated in blood flow.

5. The effect of particle density

A wide range of materials with different densities is used for drug delivery and diagnostics. Gas-filled microbubbles [93–96]

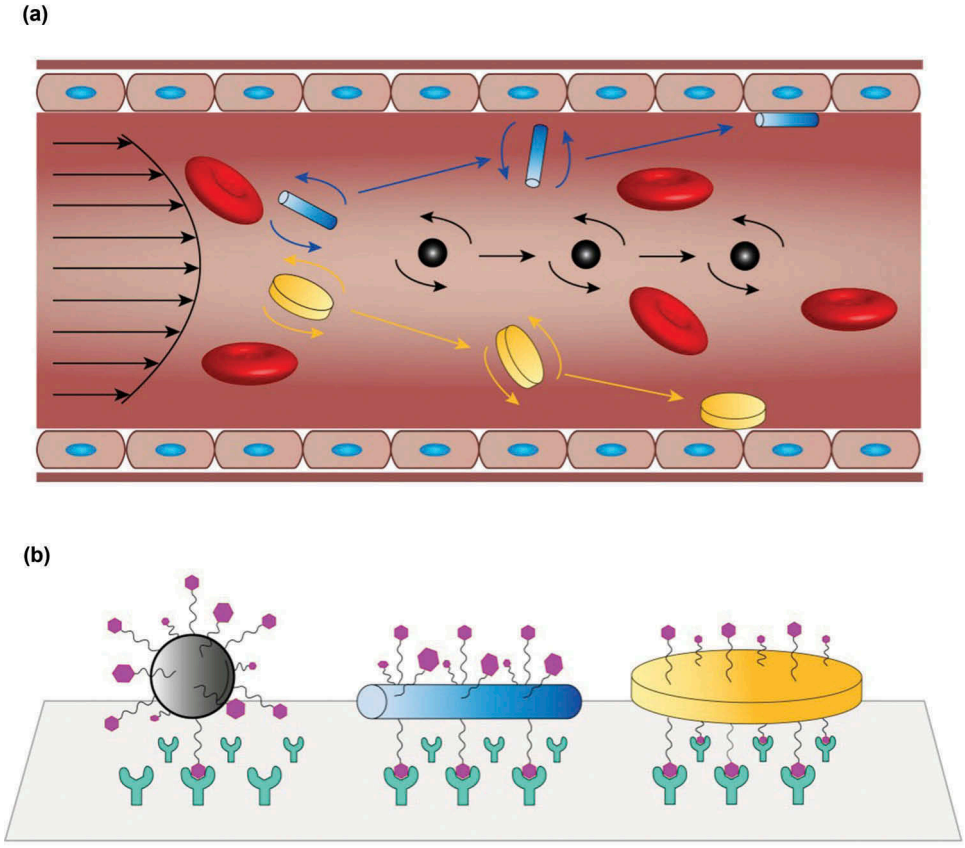

Figure 5. Effects of the morphology of the particles on their margination and binding strength (avidity). (a) Margination: Non-spherical particles such as disks and rods are subjected to torque forces within blood flow, and therefore they have a tendency to tumble out of the general circulation and scavenge along vessel walls. Spherical particles, on the other hand, tend to follow the streamlines. (b) Binding avidity: Particle elongation and flatness increase the particle surface area in contact with the endothelium and thereby present a greater number of targeting ligands to the endothelium in cases where all particles have a fixed ligand density, resulting in stronger binding strength.

have densities roughly 1% that of blood [97]. Common biocompatible and the FDA-approved polymeric particles [13,91,98,99], such as poly(lactic acid), poly(glycolic acid), poly(methyl methacrylate), polycaprolactone, and poly (lactic-co-glycolic acid), and protein-based nanoparticles tend to have densities either neutrally buoyant or slightly higher than that of blood [100,101]. Liposomes [102,103] are often neutrally buoyant but can have varied densities depending on the density of the medium encapsulated within the liposome [104,105]. Inorganic particles (e.g. silica, titanium, gold, and iron oxide) [106–109] usually have densities much higher than that of blood (silica oxide: 2.0 g ml^{-1}, titanium: 3.9 g ml^{-1}, iron oxide: 5.24 g ml^{-1}, and gold: 19.3 g ml^{-1}). Despite the wide range of densities of vascular-targeting materials, there have been limited investigations of the effect of particle density on vascular margination and adhesion. Particle density forces are usually regarded as negligible in describing particle motion relevant to physiological blood flow [25], since the hydrodynamic forces due to flow (for microparticles) and Brownian forces (for nanoparticles) are often orders of magnitude higher than density-dependent body forces such as gravitational and centrifugal forces [87].

Recently, Thompson et al. have reported the effect of material density on the margination and adhesion efficiency of particles to the vascular wall [25]. The targeting of 500-nm sLe^A-coated polystyrene, silica, and titanium nanospheres (densities of 1.05, 2.0, and 3.9 g ml^{-1}, respectively) to inflamed endothelium from human blood flow in a PPFC, an *in vitro* model of human vasculature, was investigated. Silica spheres, which have a density roughly twice that of blood, exhibited improved adhesion to inflamed endothelium compared to neutrally buoyant polystyrene spheres of the same size, in both horizontal and inverted chambers. An RBC effect was observed with silica spheres as they displayed better near-wall localization in the presence of RBCs than in pure buffer, likely resulting in the observed improvement in adhesion. Titanium spheres, which have a density around four times higher than that of blood, adhered at levels higher than polystyrene, but only in conditions where gravity or centrifugal force acted in the direction of adhesion [25]. Similar to what has been observed with polystyrene microspheres [23], both silica and titanium particles exhibited reduced adhesion efficiency as the WSR increased from 100 s^{-1} to 1000 s^{-1} [25]. In a VSFC, adhesion within the recirculation region increased for silica and titanium particles compared to polystyrene in both upright and inverted chambers. In the far downstream region, the adhesion for silica and titanium spheres was also higher than for polystyrene spheres when the chamber was upright, while there was no significant difference between particle types far downstream in the inverted chamber. However, the

improved adhesion of dense nanoparticles in recirculation flow diminished in an inverted channel. This may be because the negative gravity component overrides any benefit of the recirculation flow. The adhesion of silica and titanium in the recirculating flow pattern and further downstream was not significantly different, suggesting that the two particles were distributed to the wall area about the same amount [25].

These findings are in contrast to those of a previous study which has shown that increased density had a negative effect on the margination of nanospheres with diameters ranging from 60 to 65 nm [104]. This can be explained because the gravity component for the 65 nm spheres is negligible and the decreased margination is attributable to the increased particle momentum competing with Brownian motion toward the chamber wall. However, this study was conducted with buffer flow, not blood flow.

6. Conclusions

The physical characteristics of particles should be considered in the design of carrier systems to target atherosclerosis, as these parameters significantly affect carrier performance. Current studies show that particle size, shape, and density, along with local hemodynamic conditions including shear rate, flow type, channel height, and the presence of RBCs, all determine how well targeted carrier systems adhere to the activated endothelial cell layers or vascular walls at the sites of atherosclerosis. Regardless of shape, microparticles display better adhesion than nanoparticles. Pulsatility and recirculation in blood flow further enhance the margination of microspheres while having minimal effect on the adhesion of nanospheres. Nonspherical particles are less taken up or less cleared by macrophages and exhibit higher adhesion than their spherical counterparts. Disks perform better than rods of equivalent volume. However, no studies on the adhesion of disks to endothelial cells *in vitro* or *in vivo* have been reported. The increased density of the targeted particles also has a positive effect on the margination. These findings provide general design principles that can serve as guidelines to develop carriers for the delivery of therapeutic and imaging agents in CVD and beyond.

7. Expert opinion

Despite significant clinical advancements in the field, CVDs such as atherosclerosis remain the leading cause of death and disability worldwide. Targeting of nanomedicine to atherosclerosis can be achieved via the main lumen or the vasa vasorum at lesioned site; however, studies on the vasa vasorum in atherosclerosis targeting are limited. Although current evidence shows that nonspherical microparticles exhibit higher margination and adhesion to vascular walls under shear rates, it cannot be concluded that these particles are optimal for drug delivery in CVD. While particles with diameters on the micrometer scale have been shown to adhere more efficiently to the endothelial cell surface, they are potentially susceptible to physical entrapment in the capillaries *in vivo*. In addition, there is a lack of thorough understanding of the side effects, degradation, and toxicity of nonspherical particles at different biological levels such as the body, organs, and cells.

Nanoparticles such as nanospheres, on the other hand, have characteristics that make them attractive for use in drug delivery, including their ease of synthesis and fabrication and their capacity to undergo endocytosis and transcytosis upon contact with the endothelium. However, they are unable to efficiently marginate to the vascular wall, limiting their efficacy as a vascular-targeted carrier system for diseases affecting medium to large blood vessels such as atherosclerosis. Nevertheless, preliminary studies are encouraging for further exploration of the use of nano-constructs, as delivery systems for vascular targeting in CVD, characterized by a sub-micrometer size and a density higher than that of blood in order to maximize their near-wall accumulation within the RBC-FL while avoiding entrapment in the lungs and small capillaries and a nonspherical shape to enhance their lateral drift toward the vessel walls and their ligand–receptor interaction with the vessel walls.

Generally, the effects of particle size, shape, and density should be considered simultaneously in designing vascular-targeting carriers for CVD. Although disk-like particles exhibit higher adhesion magnitude than rod-like particles of the same volume, there has been no investigation of differences in binding in blood flow *in vitro* and *in vivo*. An important consideration associated with the use of dense materials for drug carriers in atherosclerosis is whether the high-velocity collisions of high-density particles (e.g. gold nanoparticles) with the vascular wall could potentially cause adverse effects on the endothelium itself. This is especially critical in late-stage atherosclerosis, when a significant disruption in the endothelium could potentially lead to clot formation. There is a lack of study on the role of particle's rigidity or deformable particles on vascular margination and targeting. This aspect should be investigated using nanoparticles of different rigidity but with the same chemical composition, size, and surface properties. In addition, there is a clear need for thorough studies of the cellular uptake of particles of different size, shape, and density under different flow conditions, particularly those relevant to atherosclerosis. Other shapes as well as other strategies need to be explored for improving the margination performance of nanoparticles in human blood flow, especially for application in medium to large blood vessels, which are the most relevant in CVD. Due to synthetic difficulty, spherical nanoparticles still dominate in tests and trials. Therefore, further work is needed to develop synthetic strategies to produce particles in different shapes with tunable sizes, while maintaining narrow size distributions and homogeneity. Last but not least, the effect of particle's physical properties on plaque targeting from the vasa vasorum site should be thoroughly investigated.

Funding

This work is funded by National Health and Medical Research Council [AP1037310, FT0992210], and the Australian Research Council [CE140100036].

Declaration of interest

The authors were supported by National Health and Medical Research Council and the Australian Research Council. The authors have no other relevant affiliations or financial involvement with any organization or

entity with a financial interest in or financial conflict with the subject matter or materials discussed in the manuscript apart from those disclosed.

References

Papers of special note have been highlighted as either of interest (•) or of considerable interest (••) to readers.

1. Mozaffarian D, Benjamin EJ, Go AS, et al. Heart disease and stroke statistics – 2015 update. Circulation. 2015;131:e30–e320.
2. Hajitou A, Pasqualini R, Arap W. Vascular targeting: recent advances and therapeutic perspectives. Trends Cardiovasc Med. 2006;16:80–88.
3. Psarros C, Lee R, Margaritis M, et al. Nanomedicine for the prevention, treatment and imaging of atherosclerosis. Nanomedicine. 2012;8(Suppl 1):S59–68.
4. Hansson GK. Inflammation, atherosclerosis, and coronary artery disease. N Engl J Med. 2005;352:1685–1695.
5. Gawaz M, Langer H, May AE. Platelets in inflammation and atherogenesis. J Clin Invest. 2005;115:3378–3384.
6. Falk E. Pathogenesis of atherosclerosis. J Am Coll Cardiol. 2006;47:C7–12.
   • **This is a comprehensive review on pathogenesis of atherosclerosis.**
7. Virmani R, Kolodgie FD, Burke AP, et al. Lessons from sudden coronary death: a comprehensive morphological classification scheme for atherosclerotic lesions. Arterioscler Thromb Vasc Biol. 2000;20:1262–1275.
8. Lobatto ME, Fuster V, Fayad ZA, et al. Perspectives and opportunities for nanomedicine in the management of atherosclerosis. Nat Rev Drug Discov. 2011;10:835–852.
9. Chung BL, Toth MJ, Kamaly N, et al. Nanomedicines for endothelial disorders. Nano Today. 2015;10:759–776.
10. Bicknell R. Vascular targeting and the inhibition of angiogenesis. Ann Oncol. 1994;5(Suppl 4):45–50.
11. Schnitzer JE. Vascular targeting as a strategy for cancer therapy. N Engl J Med. 1998;339:472–474.
12. Bendas G, Krause A, Schmidt R, et al. Selectins as new targets for immunoliposome-mediated drug delivery. A potential way of anti-inflammatory therapy. Pharm Acta Helv. 1998;73:19–26.
13. Muro S, Dziubla T, Qiu W, et al. Endothelial targeting of high-affinity multivalent polymer nanocarriers directed to intercellular adhesion molecule 1. J Pharmacol Exp Ther. 2006;317:1161–1169.
14. Sakhalkar HS, Dalal MK, Salem AK, et al. Leukocyte-inspired biodegradable particles that selectively and avidly adhere to inflamed endothelium in vitro and in vivo. Proc Natl Acad Sci U S A. 2003;100:15895–15900.
15. Namdee K, Thompson AJ, Golinski A, et al. In vivo evaluation of vascular-targeted spheroidal microparticles for imaging and drug delivery application in atherosclerosis. Atherosclerosis. 2014;237:279–286.
   •• **An interesting article showing effect of particle size and shape on vascular targeting *in vivo* using a mouse model of atherosclerosis.**
16. Anderson SA, Rader RK, Westlin WF, et al. Magnetic resonance contrast enhancement of neovasculature with alpha(v)beta(3)-targeted nanoparticles. Magn Reson Med. 2000;44:433–439.
17. Kiani MF, Yuan H, Chen X, et al. Targeting microparticles to select tissue via radiation-induced upregulation of endothelial cell adhesion molecules. Pharm Res. 2002;19:1317–1322.
18. Moghimi SM, Porter CJ, Muir IS, et al. Non-phagocytic uptake of intravenously injected microspheres in rat spleen: influence of particle size and hydrophilic coating. Biochem Biophys Res Commun. 1991;177:861–866.
19. Abra RM, Hunt CA. Liposome disposition in vivo. III. Dose and vesicle-size effects. Biochim Biophys Acta. 1981;666:493–503.
20. Decuzzi P, Ferrari M. The adhesive strength of non-spherical particles mediated by specific interactions. Biomaterials. 2006;27:5307–5314.
21. Decuzzi P, Pasqualini R, Arap W, et al. Intravascular delivery of particulate systems: does geometry really matter?. Pharm Res. 2009;26:235–243.
22. Park JH, von Maltzahn G, Zhang L, et al. Magnetic iron oxide nanoworms for tumor targeting and imaging. Adv Mater. 2008;20:1630–1635.
23. Charoenphol P, Huang RB, Eniola-Adefeso O. Potential role of size and hemodynamics in the efficacy of vascular-targeted spherical drug carriers. Biomaterials. 2010;31:1392–1402.
   •• **An excellent study showing effect of particle's size, hematocrit, channel orientation, channel height, wall shear rate, and flow type on vascular targeting.**
24. Charoenphol P, Mocherla S, Bouis D, et al. Targeting therapeutics to the vascular wall in atherosclerosis – carrier size matters. Atherosclerosis. 2011;217:364–370.
   • **An excellent article showing effect of particle size on vascular targeting *in vitro*.**
25. Thompson AJ, Eniola-Adefeso O. Dense nanoparticles exhibit enhanced vascular wall targeting over neutrally buoyant nanoparticles in human blood flow. Acta Biomater. 2015;21:99–108.
   •• **An article showing the effect of particle density on vascular targeting.**
26. Lee TR, Choi M, Kopacz AM, et al. On the near-wall accumulation of injectable particles in the microcirculation: smaller is not better. Sci Rep. 2013;3:2079.
27. Namdee K, Thompson AJ, Charoenphol P, et al. Margination propensity of vascular-targeted spheres from blood flow in a microfluidic model of human microvessels. Langmuir. 2013;29:2530–2535.
28. Migliorini C, Qian Y, Chen H, et al. Red blood cells augment leukocyte rolling in a virtual blood vessel. Biophys J. 2002;83:1834–1841.
29. Munn LL, Melder RJ, Jain RK. Role of erythrocytes in leukocyte-endothelial interactions: mathematical model and experimental validation. Biophys J. 1996;71:466–478.
30. Hammer DA. Leukocyte adhesion: what's the catch?. Curr Biol. 2005;15:R96–9.
31. Sun C, Migliorini C, Munn LL. Red blood cells initiate leukocyte rolling in postcapillary expansions: a lattice Boltzmann analysis. Biophys J. 2003;85:208–222.
32. Nobis U, Pries AR, Cokelet GR, et al. Radial distribution of white cells during blood flow in small tubes. Microvasc Res. 1985;29:295–304.
33. Guyton AC, Hall JE. Textbook of medical physiology. 11th ed. Philadelphia: Elsevier, Inc.; 2006.
34. Chiu JJ, Chien S. Effects of disturbed flow on vascular endothelium: pathophysiological basis and clinical perspectives. Physiol Rev. 2011;91:327–387.
   •• **An interesting review on blood flow in pathophysiological conditions.**
35. Atukorale PU, Covarrubias G, Bauer L, et al. Vascular targeting of nanoparticles for molecular imaging of diseased endothelium. Adv Drug Deliv Rev. 2016. doi: 10.1016/j.addr.2016.09.006
36. Stone PH, Saito S, Takahashi S, et al. Prediction of progression of coronary artery disease and clinical outcomes using vascular profiling of endothelial shear stress and arterial plaque characteristics: the PREDICTION Study. Circulation. 2012;126:172–181.
   •• **An excellent study on blood flow and its effect on progression of coronary artery disease.**
37. Ku DN, Giddens DP, Zarins CK, et al. Pulsatile flow and atherosclerosis in the human carotid bifurcation. Positive correlation between plaque location and low oscillating shear stress. Arteriosclerosis. 1985;5:293–302.
38. Thompson AJ, Mastria EM, Eniola-Adefeso O. The margination propensity of ellipsoidal micro/nanoparticles to the endothelium in human blood flow. Biomaterials. 2013;34:5863–5871.
39. Huang RB, Mocherla S, Heslinga MJ, et al. Dynamic and cellular interactions of nanoparticles in vascular-targeted drug delivery. Mol Membr Biol. 2010;27:312–327.
40. Adriani G, De Tullio MD, Ferrari M, et al. The preferential targeting of the diseased microvasculature by disk-like particles. Biomaterials. 2012;33:5504–5513.
   • **An article showing better adhesion of disk-like particles compared to rods.**
41. Charoenphol P, Onyskiw PJ, Carrasco-Teja M, et al. Particle-cell dynamics in human blood flow: implications for vascular-targeted drug delivery. J Biomech. 2012;45:2822–2828.

42. Sharan M, Popel AS. A two-phase model for flow of blood in narrow tubes with increased effective viscosity near the wall. Biorheology. 2001;38:415–428.
43. Koutsiaris AG, Tachmitzi SV, Batis N, et al. Volume flow and wall shear stress quantification in the human conjunctival capillaries and post-capillary venules in vivo. Biorheology. 2007;44:375–386.
44. Nagaoka T, Yoshida A. Noninvasive evaluation of wall shear stress on retinal microcirculation in humans. Invest Ophthalmol Vis Sci. 2006;47:1113–1119.
45. Tilles AW, Eckstein EC. The near-wall excess of platelet-sized particles in blood flow: its dependence on hematocrit and wall shear rate. Microvasc Res. 1987;33:211–223.
46. Eckstein EC, Tilles AW, Millero FJ. Conditions for the occurrence of large near-wall excesses of small particles during blood flow. Microvasc Res. 1988;1:31–39.
47. Abbitt KB, Nash GB. Characteristics of leucocyte adhesion directly observed in flowing whole blood in vitro. Br J Haematol. 2001;112:55–63.
48. Kim S, Kong RL, Popel AS, et al. Temporal and spatial variations of cell-free layer width in arterioles. Am J Physiol Heart Circ Physiol. 2007;293:H1526–35.
49. Pappu V, Bagchi P. Hydrodynamic interaction between erythrocytes and leukocytes affects rheology of blood in microvessels. Biorheology. 2007;44:191–215.
50. Shinde Patil VR, Campbell CJ, Yun YH, et al. Particle diameter influences adhesion under flow. Biophys J. 2001;80:1733–1743.
51. Chang KC, Hammer DA. The forward rate of binding of surface-tethered reactants: effect of relative motion between two surfaces. Biophys J. 1999;76:1280–1292.
52. Slack SM, Turitto VT. Fluid dynamic and hemorheologic considerations. Cardiovasc Pathol. 1993;2:11S–21S.
53. Kim S, Ong PK, Yalcin O, et al. The cell-free layer in microvascular blood flow. Biorheology. 2009;46:181–189.
54. Maeda N, Suzuki Y, Tanaka J, et al. Erythrocyte flow and elasticity of microvessels evaluated by marginal cell-free layer and flow resistance. Am J Physiol. 1996;271:H2454–61.
55. Decuzzi P, Ferrari M. Design maps for nanoparticles targeting the diseased microvasculature. Biomaterials. 2008;29:377–384.
56. Skilbeck C, Westwood SM, Walker PG, et al. Dependence of adhesive behavior of neutrophils on local fluid dynamics in a region with recirculating flow. Biorheology. 2001;38:213–227.
57. Skilbeck CA, Walker PG, David T, et al. Disturbed flow promotes deposition of leucocytes from flowing whole blood in a model of a damaged vessel wall. Br J Haematol. 2004;126:418–427.
58. Chiu JJ, Chen CN, Lee PL, et al. Analysis of the effect of disturbed flow on monocytic adhesion to endothelial cells. J Biomech. 2003;36:1883–1895.
59. Less JR, Skalak TC, Sevick EM, et al. Microvascular architecture in a mammary carcinoma: branching patterns and vessel dimensions. Cancer Res. 1991;51:265–273.
60. Champion JA, Karate YK, Samir M. Particle shape: a new design parameter for micro- and nanoscale drug delivery carriers. J Control Release. 2007;121:1–2.
61. Truong NP, Whittaker MR, Mak CW, et al. The importance of nanoparticle shape in cancer drug delivery. Expert Opin Drug Deliv. 2015;12:129–142.
62. Champion JA, Mitragotri S. Role of target geometry in phagocytosis. Proc Natl Acad Sci U S A. 2006;103:4930–4934.
63. Gratton SE, Ropp PA, Pohlhaus PD, et al. The effect of particle design on cellular internalization pathways. Proc Natl Acad Sci U S A. 2008;105:11613–11618.
64. Huang X, Li L, Liu T, et al. The shape effect of mesoporous silica nanoparticles on biodistribution, clearance, and biocompatibility in vivo. ACS Nano. 2011;5:5390–5399.
65. Arnida, Janat-Amsbury MM, Ray A, et al. Geometry and surface characteristics of gold nanoparticles influence their biodistribution and uptake by macrophages. Eur J Pharm Biopharm. 2011;77:417–423.
66. Geng Y, Dalhaimer P, Cai S, et al. Shape effects of filaments versus spherical particles in flow and drug delivery. Nat Nanotechnol. 2007;2:249–255.
67. Muro S, Garnacho C, Champion JA, et al. Control of endothelial targeting and intracellular delivery of therapeutic enzymes by modulating the size and shape of ICAM-1-targeted carriers. Mol Ther. 2008;16:1450–1458.
• **An interesting article on prolonged circulation and cellular uptake of elliptical disks.**
68. Truong NP, Quinn JF, Whittaker MR, et al. Polymeric filomicelles and nanoworms: two decades of synthesis and application. Polym Chem. 2016;7:4295–4312.
69. Champion JA, Mitragotri S. Shape induced inhibition of phagocytosis of polymer particles. Pharm Res. 2009;26:244–249.
•• **An interesting article on cellular uptake of rod- or worm-like particles.**
70. Huang X, Teng X, Chen D, et al. The effect of the shape of mesoporous silica nanoparticles on cellular uptake and cell function. Biomaterials. 2010;31:438–448.
71. Chithrani BD, Ghazani AA, Chan WC. Determining the size and shape dependence of gold nanoparticle uptake into mammalian cells. Nano Lett. 2006;6:662–668.
72. Liu X, Wu F, Tian Y, et al. Size dependent cellular uptake of rod-like bionanoparticles with different aspect ratios. Sci Rep. 2016;6:24567.
73. Doshi N, Prabhakarpandian B, Rea-Ramsey A, et al. Flow and adhesion of drug carriers in blood vessels depend on their shape: a study using model synthetic microvascular networks. J Control Release. 2010;146:196–200.
• **An article showing that rod-shaped particles exhibited significantly higher vascular attachment compared to spherical particles.**
74. Gentile F, Chiappini C, Fine D, et al. The effect of shape on the margination dynamics of non-neutrally buoyant particles in two-dimensional shear flows. J Biomech. 2008;41:2312–2318.
75. Liang S, Slattery MJ, Wagner D, et al. Hydrodynamic shear rate regulates melanoma-leukocyte aggregation, melanoma adhesion to the endothelium, and subsequent extravasation. Ann Biomed Eng. 2008;36:661–671.
76. Jain RK, Stylianopoulos T. Delivering nanomedicine to solid tumors. Nat Rev Clin Oncol. 2010;7:653–664.
77. Peiris PM, Toy R, Doolittle E, et al. Imaging metastasis using an integrin-targeting chain-shaped nanoparticle. ACS Nano. 2012;6:8783–8795.
78. Peiris PM, Schmidt E, Calabrese M, et al. Assembly of linear nanochains from iron oxide nanospheres with asymmetric surface chemistry. Plos One. 2011;6:e15927.
79. Peiris PM, Bauer L, Toy R, et al. Enhanced delivery of chemotherapy to tumors using a multicomponent nanochain with radio-frequency-tunable drug release. ACS Nano. 2012;6:4157–4168.
80. Peiris PM, Tam M, Vicente P, et al. On-command drug release from nanochains inhibits growth of breast tumors. Pharm Res. 2014;31:1460–1468.
81. Peiris PM, Toy R, Abramowski A, et al. Treatment of cancer micrometastasis using a multicomponent chain-like nanoparticle. J Control Release. 2014;173:51–58.
82. Peiris PM, Abramowski A, McGinnity J, et al. Treatment of invasive brain tumors using a chain-like nanoparticle. Cancer Res. 2015;75:1356–1365.
83. Peiris PM, Deb P, Doolittle E, et al. Vascular targeting of a gold nanoparticle to breast cancer metastasis. J Pharm Sci. 2015;104:2600–2610.
84. Simone E, Ding BS, Muzykantov V. Targeted delivery of therapeutics to endothelium. Cell Tissue Res. 2009;335:283–300.
85. Champion JA, Katare YK, Mitragotri S. Making polymeric micro- and nanoparticles of complex shapes. Proc Natl Acad Sci U S A. 2007;104:11901–11904.
86. Backer MV, Gaynutdinov TI, Patel V, et al. Vascular endothelial growth factor selectively targets boronated dendrimers to tumor vasculature. Mol Cancer Ther. 2005;4:1423–1429.
87. Lee SY, Ferrari M, Decuzzi P. Shaping nano-/micro-particles for enhanced vascular interaction in laminar flows. Nanotechnology. 2009;20:495101.
88. Truong NP, Whittaker MR, Anastasaki A, et al. Facile production of nanoaggregates with tuneable morphologies from thermoresponsive P(DEGMA-co-HPMA). Polym Chem. 2016;7:430–440.

89. Wen AM, Wang Y, Jiang K, et al. Shaping bio-inspired nanotechnologies to target thrombosis for dual optical-magnetic resonance imaging. J Mater Chem B Mater Biol Med. 2015;3:6037–6045.
90. Kolhar P, Anselmo AC, Gupta V, et al. Using shape effects to target antibody-coated nanoparticles to lung and brain endothelium. Proc Natl Acad Sci U S A. 2013;110:10753–10758.
91. Shuvaev VV, Ilies MA, Simone E, et al. Endothelial targeting of antibody-decorated polymeric filomicelles. ACS Nano. 2011;5:6991–6999.
92. Gavze E, Shapiro M. Motion of inertial spheroidal particles in a shear flow near a solid wall with special application to aerosol transport in microgravity. J Fluid Mech. 1998;371:59–79.
• **A study using modeling to investigate the effect of particle's shape on vascular targeting.**
93. Unger E, Porter T, Lindner J, et al. Cardiovascular drug delivery with ultrasound and microbubbles. Adv Drug Deliv Rev. 2014;72:110–126.
94. Ting CY, Fan CH, Liu HL, et al. Concurrent blood-brain barrier opening and local drug delivery using drug-carrying microbubbles and focused ultrasound for brain glioma treatment. Biomaterials. 2012;33:704–712.
95. Wang X, Gkanatsas Y, Palasubramaniam J, et al. Thrombus-targeted theranostic microbubbles: a new technology towards concurrent rapid ultrasound diagnosis and bleeding-free fibrinolytic treatment of thrombosis. Theranostics. 2016;6:726–738.
96. Wang X, Hagemeyer CE, Hohmann JD, et al. Novel single-chain antibody-targeted microbubbles for molecular ultrasound imaging of thrombosis: validation of a unique noninvasive method for rapid and sensitive detection of thrombi and monitoring of success or failure of thrombolysis in mice. Circulation. 2012;125:3117–3126.
97. Takalkar AM, Klibanov AL, Rychak JJ, et al. Binding and detachment dynamics of microbubbles targeted to P-selectin under controlled shear flow. J Control Release. 2004;96:473–482.
98. Nance E, Zhang C, Shih TY, et al. Brain-penetrating nanoparticles improve paclitaxel efficacy in malignant glioma following local administration. ACS Nano. 2014;8:10655–10664.
99. Kamaly N, Xiao Z, Valencia PM, et al. Targeted polymeric therapeutic nanoparticles: design, development and clinical translation. Chem Soc Rev. 2012;41:2971–3010.
100. Koo OM, Rubinstein I, Onyuksel H. Role of nanotechnology in targeted drug delivery and imaging: a concise review. Nanomedicine. 2005;1:193–212.
101. Kim W, Haller C, Dai E, et al. Targeted antithrombotic protein micelles. Angew Chem Int Ed Engl. 2015;54:1461–1465.
102. Allen TM. Long-circulating (sterically stabilized) liposomes for targeted drug delivery. Trends Pharmacol Sci. 1994;15:215–220.
103. Allen TM, Cullis PR. Liposomal drug delivery systems: from concept to clinical applications. Adv Drug Deliv Rev. 2013;65:36–48.
104. Toy R, Hayden E, Shoup C, et al. The effects of particle size, density and shape on margination of nanoparticles in microcirculation. Nanotechnology. 2011;22:115101.
105. Singh AK, Cummings EB, Throckmorton DJ. Fluorescent liposome flow markers for microscale particle-image velocimetry. Anal Chem. 2001;73:1057–1061.
106. Liong M, Lu J, Kovochich M, et al. Multifunctional inorganic nanoparticles for imaging, targeting, and drug delivery. ACS Nano. 2008;2:889–896.
107. Huang HC, Barua S, Sharma G, et al. Inorganic nanoparticles for cancer imaging and therapy. J Control Release. 2011;155:344–357.
108. Tom RT, Suryanarayanan V, Reddy PG, et al. Ciprofloxacin-protected gold nanoparticles. Langmuir. 2004;20:1909–1914.
109. Ta HT, Prabhu S, Leitner E, et al. Enzymatic single-chain antibody tagging: a universal approach to targeted molecular imaging and cell homing in cardiovascular disease. Circ Res. 2011;109:365–373.